Earth's Future

RESEARCH ARTICLE
10.1029/2025EF007435

Special Collection:
Transdisciplinary Collaboration for Sustainable Agriculture

Key Points:

- Reducing N in high-fertility soils shows a strong resistance for global crop production
- Resupplying N in low-fertility soils can achieve high yields with rational N surplus
- The study provides a model for sustainable flexible management in different historical management regions

Supporting Information:

Supporting Information may be found in the online version of this article.

Correspondence to:

X. Ju,
juxt@cau.edu.cn

Citation:

Tian, X., Cao, R., Liu, X., Li, Y., Wang, Z., Zhang, C., et al. (2026). Resistance and recovery of crop productivity from contrasted soil fertility. *Earth's Future*, *14*, e2025EF007435. https://doi.org/10.1029/2025EF007435

Received 10 OCT 2025
Accepted 20 MAY 2026

Author Contributions:

Conceptualization: Xiaotang Ju
Data curation: Xue Tian, Rui Cao, Xinyuan Liu, Yue Li, Zhujun Wang
Formal analysis: Xue Tian
Funding acquisition: Chong Zhang, Xiaotang Ju
Investigation: Xue Tian, Rui Cao, Xinyuan Liu, Yue Li
Methodology: Xiaotang Ju
Project administration: Xiaotang Ju
Supervision: Xiaotang Ju
Visualization: Xue Tian
Writing – original draft: Xue Tian

Resistance and Recovery of Crop Productivity From Contrasted Soil Fertility

Xue Tian[1], Rui Cao[1], Xinyuan Liu[1], Yue Li[2], Zhujun Wang[1], Chong Zhang[1], Xiaotong Song[3], Di Wu[2], Robert M. Rees[4], Klaus Butterbach-Bahl[5,6], and Xiaotang Ju[1]

[1]School of Tropical Agriculture and Forestry, Hainan University, Haikou, China, [2]CAS Key Laboratory of Forest Ecology and Silviculture, Institute of Applied Ecology, Chinese Academy of Sciences, Shenyang, China, [3]Research Center for Eco-Environmental Sciences, Chinese Academy of Sciences, Beijing, China, [4]SRUC, Edinburgh, UK, [5]Institute of Meteorology and Climate Research, Atmospheric Environmental Research (IMK-IFU), Karlsruhe Institute of Technology (KIT), Garmisch-Partenkirchen, Germany, [6]Department of Agroecology, Pioneer Center Land-CRAFT, Aarhus University, Aarhus, Denmark

Abstract The balance between crop production and environmental sustainability depends on an adequate supply of soil nutrients, although changes in nutrient supply may initially have little effect on crop production due to the buffering effects of soil nutrients and the overall resilience of the system. In a 15-year fertilizer experiment in the North China Plain, crop yield on high-fertility soils declined little in the first year after N application was stopped, indicating a strong resilience (0.90) caused by the mining of previously accumulated soil N. Restoration of manure N at a reduced rate resulted in an immediate yield increase of 136% and increased the N surplus to 134 kg N ha^{-1}. A synthesis of the literature showed that global soils also have a high yield resilience (0.94–1.00). This work suggests that in low-fertility soils, N resupply can contribute to rapidly increase yields under optimum management, thereby aiding efforts to address rising food demand. Conversely, in high fertility soils (high residual N), reduced N applications can maintain high yields with reduced N losses.

Plain Language Summary Croplands with an excess or deficiency of nitrogen fertilization faces challenges in balancing production and environmental sustainability. However, the impact of soil nutrient supply from historical managements on crop production and the environment remains unclear. The study provides an insight into sustainable food production practices, emphasizing the significance of flexible management in specific regions with different N management histories for food security and environmental sustainability. For instance, in regions such as China and India with long-term high-N input soil, the cessation of N application in the short term can maintain high yields while reducing N environmental risks. Furthermore, it can bolster confidence in poor soil in sub-Saharan Africa, restoring N application can rapidly enhance crop yield while reducing soil N mining to maintain the environmental friendliness. Flexible management strategies will help achieve greater productivity and environmental performance, delivering multiple benefits for both humans and the environment.

1. Introduction

Sustainable food production to feed a growing world population at a lower environmental cost is a major challenge for agriculture and humanity (Foley et al., 2011; Steffen et al., 2015). Nitrogen (N) fertilization has been responsible for feeding nearly half of the world's population since the invention of the Haber-Bosch process (Erisman et al., 2008). It has been argued that global food production will need to increase by 30%–62% between 2010 and 2050 to meet the demands of food security and sustainability under climate change (Hasegawa et al., 2021; van Dijk et al., 2021). However, the overuse of N fertilizers has contributed to negative impacts on crop yields and incomes, with major environmental impacts (Battye et al., 2017; Bodirsky et al., 2014), as for example, agriculture is responsible for 90% of anthropogenic ammonia (NH_3) and ~60% of anthropogenic nitrous oxide (N_2O) emissions in China (Tian et al., 2024; Zhan et al., 2020). Recognizing the urgent problem, major economies have enacted targeted policies, such as the European Union's Farm to Fork strategy and China's zero growth of fertilizer Action. Meanwhile, the "underuse" of N fertilizers has led to lower crop yields and soil N depletion in certain areas, such as sub-Saharan Africa (Smerald et al., 2023). The global challenge is therefore to address these two opposing issues to increase crop yields while improving soil environmental sustainability in the context of either excessive or insufficient N use (Stevens, 2019).

Writing – review & editing: Chong Zhang, Xiaotong Song, Di Wu, Robert M. Rees, Klaus Butterbach-Bahl, Xiaotang Ju

It is likely that target locations for increasing crop yields will be on deficient-N soils, as is the case in many parts of Africa (FAO et al., 2024), where yields are currently well below average (Smerald et al., 2022). Likewise, the location for mitigating environmental problems is likely to be found where soils receive excessive N inputs such as those in many parts of North America, Europe and East Asia, where high yields often coincide with the negative environmental impacts (Smerald et al., 2023; Stevens, 2019; Wang et al., 2022). The causes of low yield regions are often primarily due to nutrient limitations (FAO et al., 2024; Foley et al., 2011). It is therefore possible to achieve higher yields without environmental risk by increasing nutrient inputs (Foley et al., 2011). Soils are conditioned by past management practices (Rahmati et al., 2023), but the response of crops to past N deficits (i.e., recovery) remains unclear. At the other end of the spectrum, a legacy effect persists for long periods of time in the residual soil N pool resulting from high N fertilization, which can be used by crops or lost to the environment (Sebilo et al., 2013). However, little is known about the extent and duration of the legacy of historical N management in crops (i.e., resistance). Therefore, we explored the effects of recovery and resistance from contrasting soil fertility backgrounds to identify site-specific best management practices that provide optimal yield with minimal environmental impact.

A long-term field experiment based on different soil fertility backgrounds was used as a platform for this study. The experimental site in the North China Plain (NCP) had been cultivated for 15 years with contrasting carbon and N management treatments. The cropping system was double cropped with winter wheat (Triticum aestivum L.) and summer maize (Zea mays L.), which account for about 75% and 35% of China's total wheat and maize production, respectively (NBSC, 2023). We first examined crop productivity under both long-term fertilization regimes and after N conversion, referred to as the ‘original’ and ‘conversion’ scenarios, respectively. We then evaluated: (a) resistance on historically high-fertility soils, defined as a scenario in which crop production reaches a normal high level following the cessation of N fertilization; and (b) recovery on historical low and medium fertility soils, defined as the effect of returning to a high level of crop production following an increase in N supply. The high level of crop production was not static, but refers to the high yield and high N uptake that are affected by interannual weather variations in the NCP. Our hypotheses were that (a) the high N fertility soil would exhibit resistance resulting in a buffering of changes in crop productivity following cessation of N applications, and (b) the low N fertility soil would exhibit a rapid recovery in crop yield following reapplication of N fertilizer after a period of cessation. We demonstrate that there was strong resistance in crop production and the environmental benefits in the first year following removal of N application on high fertility soils, and strong recovery in crop production and the environmental benefits following restoration of N applications on low fertility soils. The results show that strong resistance and recovery can provide guidance toward national targets for site-specific best management practices for sustainable agriculture under different soil conditions.

2. Materials and Methods

2.1. Study Site and Experimental Design

The field experiment was located at the Shangzhuang Experimental Station of China Agricultural University in Beijing (40°8.40′N, 116°10.80′E) in the North China Plain (NCP). The region has a typical continental monsoon climate with a mean annual precipitation of 500–700 mm, mainly from July to September and a mean annual temperature of 13.0°C. The soil was classified as a Calcaric Ochri-Aquic Cambisol according to the Chinese Soil Taxonomy (Institute of Soil Science). The main cropping system is a typical rotation cycle of winter wheat (*Triticum aestivum* L.) and summer maize (*Zea mays* L.) in the NCP, in which winter wheat is sown in early October and harvested in mid-June the following year, and then summer maize is planted immediately after harvesting the winter wheat and harvested at the beginning of October. The topsoil (0–20 cm), a clay loam texture with 28% clay, 32% silt and 40% sand (USDA standard), contained 7.7 g kg^{-1} soil organic C (SOC), 0.8 g kg^{-1} total N (TN), 24.5 mg kg^{-1} nitrate N (NO_3^--N), 1.2 mg kg^{-1} ammonium N (NH_4^+-N), 7.8 mg kg^{-1} available phosphorus (P), and 76.2 mg kg^{-1} available potassium (K) with a soil bulk density of 1.31 g cm^{-3} and pH of 8.1.

The study was based on a long-term field experiment established in October 2006 with eight treatments: four N application rates [zero N (N_0), optimal synthetic N (N_{opt}), conventional synthetic N (N_{con}), and balanced mineral N with manure (MN_{bal})], each with return (S) and removal of all straw to the field. The trial was arranged in randomized blocks with three replications with a total of 24 plots (8 m × 8 m). The eight treatments were as follows: N_0 and SN_0 as control, no N fertilizer input with and without straw; N_{opt} and SN_{opt}, synthetic N applied at the rates of 160 kg N ha^{-1} for wheat and maize with and without straw, according to the mineral N (N_{min}) test from

2006 to 2011; N_{con} and SN_{con}, synthetic N input at the rates of 300 and 260 kg N ha^{-1} for wheat and maize with and without straw, respectively; MN_{bal} and SMN_{bal}, the total of 170 and 180 kg N ha^{-1} for wheat and maize with and without straw, respectively, composted cow manure applied with supplementary synthetic N fertilizer based on the N balanced calculations during 2006–2011, that is, the sum of the target N supply of wheat and maize and the remaining soil residual mineral N was divided into synthetic N, available manure N, and initial soil mineral N.

This study used a blocked split-plot design by converting the long-term regimes from October 2020 to October 2023. Physical and chemical properties of soil samples from the different experimental treatments are shown in Table S1 of Supporting Information S1. Each long-term plot was subdivided into original (8 m × 3 m) and conversion (8 m × 5 m) sub-plots (Figure S1 in Supporting Information S1). The original sub-plots were the same as the regimes of the long-term field trial. The conversion sub-plots were converted based the regimes of the long-term experiment, which included two N fertilizer rates (zero N and manure with mineral N) and two straw managements (straw return and removal). The conversion treatments were: (a) NN, converted to zero N applications with straw removal on the original SN_{con} and SMN_{bal} plots; (b) NNS, converted to zero N application with straw return on the original of N_{con} and MN_{bal} plots; (c) MN, converted to manure with mineral N fertilizer with straw removal on the original SN_0 and SN_{opt} plots; (d) MNS, converted to manure with mineral N fertilizer with straw return on the original N_0 and N_{opt} plots. The N treatments of the MN and MNS were similar to the MN_{bal} and SMN_{bal}. Other fertilizers and agronomic management remained the same in the original and conversion plots with the historical regimes of the long-term field trial.

Nitrogen fertilizer was applied in the form of urea, divided into basal fertilizer (one-third) and topdressing at elongation (two-third) in winter wheat, while the ratio of summer maize was 1:1 at four-leaf and ten-leaf stage. 100 kg P_2O_5/K_2O ha^{-1} of synthetic P and K fertilizers was applied in two dressings for all sub-plots. An additional 30 kg $ZnSO_4$ ha^{-1} was applied at the four-leaf stage of maize. There were ∼5 irrigation events during the wheat season, and one (60 mm) immediately after sowing to favor seedling emergence during the maize season. The seeding density was 225 kg ha^{-1} for wheat and 66,667 plants ha^{-1} for maize, which is comparable to the typical practice in the NCP.

2.2. Crop Production, Conversion Effect and N Surplus

Fresh aboveground wheat was harvested in the middle of each plot measuring 4.5 m^2 (3 m × 1.5 m) from a conversion sub-plot and 6.0 m^2 (3 m × 2 m) from an original sub-plot. Then grain and straw samples were obtained and oven-dried at 70°C for the grain and straw biomass. At the maize maturity, the aboveground plant from 10.8 m^2 (1.8 m × 6 m, three rows 6 m in length) and 12.0 m^2 (3 m × 4 m, five rows 4 m in length) in the middle of each plot was harvested measuring the ear number of one and two rows among these from the original and conversion sub-plots respectively. Five plants were randomly selected from the harvested maize, and divided into grain, straw, and cob to determine the biomass by oven-drying at 70°C. The components of wheat and maize were manually crushed and their N content measured by a Vario MACRO CN (Elementar Analysensysteme GmbH, Hessian, Germany).

To compare the differences between the original and the conversion, the conversion effect (%) was estimated as follows:

$$\text{Conversion effect}_{ij} = \frac{\text{Conversion}l_j^i - \text{Original}_j^i}{\text{Original}_j^i} \tag{1}$$

where conversion and original indicate the conversion and original sub-plot; i represents the season that is, 1st wheat, 2nd maize, 3rd wheat, 4th maize, 5th wheat, and 6th maize; j indicates the crop aboveground biomass and N uptake.

N surplus, as an indicator for evaluating N management, was calculated as the difference between total N inputs and the N outputs. The main external N inputs were fertilizer N, manure N, straw N, atmospheric deposition N, biological N_2 fixation, irrigation N and seed N. Internal N cycling, net soil organic N mineralization, was not taken into account. N output contains the harvested crop N.

$$N_{sur} = N_{fer} + N_{man} + N_{str} + N_{dep} + N_{fix} + N_{irr} + N_{see} - N_{har} \tag{2}$$

where N_{sur} is N surplus; N_{fer}, N_{man}, N_{str}, N_{dep}, N_{fix}, N_{irr}, and N_{see} represents the N input from fertilizer, manure, straw, atmospheric deposition, biological N fixation, irrigation, and seed, respectively; N_{har} is the N output in grain and straw (and cob for maize only). However, it does not account for N immobilization or specific loss pathways, such as ammonia volatilization, nitrate leaching, surface runoff, and reactive gas emissions. The apparent N surplus serves as a relative indicator when direct, comprehensive quantification of all individual N losses is impractical at large scales or in long-term studies.

Atmospheric deposition N ranged from 32.0 to 35.6 kg N ha^{-1} yr^{-1} in NCP (Wen et al., 2020). N deposition during the wheat and maize growing seasons was calculated separately, from the wheat season which accounts for 39% (ranged from 36% to 44%) of the total annual N deposition (Liu et al., 2019). Biological N_2 fixation was estimated to be 5 kg N ha^{-1} for both wheat and maize (Bouwman et al., 2013). Irrigation N was calculated as 9.1–10.3 kg N ha^{-1} in the winter wheat season and 2.3 kg N ha^{-1} in the summer corn season by calculating the N concentration in the water and the total amount of irrigation (240–270 mm for wheat season and 60 mm for maize season). Seed carrying N was 4.7 and 0.7 kg N ha^{-1} calculated by the 225 and 44 kg ha^{-1} of the sowing rates for wheat and maize with their N contents.

2.3. Resistance and Recovery Index

Resistance indicates the proximity of crop aboveground biomass and N uptake to a normal (original) level after a fertilizer application was stopped. Recovery refers to the effect of return toward a normal high level for crop aboveground biomass and N uptake after a fertilizer re-application. The adapted resistance and recovery indices were calculated as follows (Chaer et al., 2009; Kaufman, 1982):

$$\text{Resistance index}_{ij} = \log_{10}\left(10 \times \frac{\text{Conversion}_j^i}{\text{Original}_j^i}\right) \tag{3}$$

$$\text{Recovery index}_{ij} = \log_{10}\left(10 \times \frac{\text{Conversion}_j^i}{\Upsilon_j^i}\right) \tag{4}$$

where conversion and original indicate the conversion and original sub-plot; i represents the season that is, 1st wheat, 2nd maize, 3rd wheat, 4th maize, 5th wheat, and 6th maize; j indicates the crop aboveground biomass and N uptake; Υ indicates the average of the conventional N and balanced N at the original. Resistance occurs only for long term conventional N and balanced mineral N with manure, while recovery occurs only for zero N and optimal N before conversion.

Taking the N effects of the zero N and optimal N into account to direct the difference in recovery:

$$\text{Original N effects} = \log_{10}\left(10 \times \frac{\text{Original}_j^i}{\Upsilon_j^i}\right) \tag{5}$$

2.4. Soil Environmental Variables

At the maize harvest each October, fresh soil samples were taken from the top 100 cm of the soil profile from four points in each sub-plot using a soil auger. Soil samples from each 20 cm layer were mixed thoroughly and passed through a 2 mm sieve. The fresh soil samples of five layers were extracted with 1.0 M KCl solution to determine the concentrations of NH_4^+-N and NO_3^--N by a Microplate Reader (TECAN_infinite F50, Männedorf, ZH, Switzerland). Soil pH, moisture, organic carbon (SOC), total N (TN), available P (AP) and available K (AK) were also measured in the 0–60 cm (top three layers) soils after air-dried. Soil pH was assessed in a 1:5 (w/v) soil: water suspension using a pH meter. Soil moisture was measured by the gravimetric method after samples were oven-dried at 105°C for 24 hr. SOC was determined calorimetrically following oxidation with a combination of potassium dichromate and sulfuric acid. TN was determined using the Kjeldahl method. AP and AK concentrations were extracted by 0.5 M $NaHCO_3$ (pH 8.5) and 1.0 M NH_4OAc (pH 7) and measured by molybdenum blue colorimetric and flame photometer method, respectively.

2.5. DNA Extraction and High-Throughput Sequencing

Composite surface soil samples (top ∼20 cm depth) were mixed by taking five soil cores at each plot on 24 July 2022, during the crop growing season. Soil samples were sieved through a 2.0 mm mesh to remove plant roots, litter, rocks, and other debris. Each soil sample was frozen at −80°C for DNA extraction and microbial analysis.

Total genomic DNA was extracted from 0.5 g of fresh soil using the Powersoil DNA Isolation Kit (Mo Bio Laboratories, Carlsbad, CA, USA) following the manufacturer's instructions. The extracted DNA was quantified and qualified using a Nanodrop ONE spectrophotometer (NanoDrop Technologies, Wilmington, DE, USA). Amplicon sequencing was used to quantify the abundance of 16S rRNA and ITS using a BioRad S1000 (Bio-Rad Laboratory, CA, USA). The bacterial 16S rRNA genes were amplified the V4 region using the primer pairs 515F/806R (5′-GTGCCAGCMGCCGCGGTAA-3′/5′-GCACTACHVGGGTWTCTAAT-3′). For the fungal community, ITS2 region was amplified using primers 5.8S-Fun/ITS4-Fun (5′-AACTTTYRRCAAYGGATCWCT - 3′/5′-AGCCTCCGCTTATTGATATGCTTAART-3′), targeting the ITS2-4 region. A polymerase chain reaction (PCR) was performed with 50 μL reaction volumes: 25 μL 2x Premix Taq (Takara Biotechnology), 1 μL 10 μM primer-F, 1 μL 10 μM primer-R, 50 ng DNA template, and 22 μL ddH_2O. The PCR thermal cycling condition was 95°C for 2 min, followed by 30 cycles of 95°C for 20 s, 53°C for 20 s and 72°C for 20 s with a final extension at 72°C for 5 min. Each sample was replicated three times, and the specificity of PCR amplification was determined by resolution curve analysis.

The taxonomic profiles of soil bacterial and fungal communities were determined via high-throughput sequencing using the Illumina MiSeq platform (Illumina, San Diego, CA, USA). The sequence processing procedure, inclusive of quality control and splicing, was conducted via an analytical pipeline that integrated the requisite bioinformatics tools (Feng et al., 2017). High-quality sequences were then clustered into operational taxonomic units (OTUs) at the 97% similarity threshold using the UPARSE algorithm (Edgar, 2013), and chimeras were eliminated during this procedure. Taxonomic assignments were carried out using OTUs with SILVA (for bacteria) and UNITE (for fungi). The sequence number in each sample was rarefied to the same depth for the 16S rRNA gene (84,277 reads) or ITS sequences (66,474 reads), leaving a total of 22,445 bacterial OTUs and 2,138 fungal OTUs for further analyses.

2.6. Literature Synthesis

We gathered a global observation data set consisting of 161 resistance indexes and 47 recovery indexes from currently peer-reviewed publications (Supplementary Methods). In addition to calculating based on the "Normal" value presented in the article, the resistance and recovery indices of crop yield were also calculated based on the global crop potential yield (attainable yield). Crop potential yields were extracted from Mueller et al. (2012) using site latitudes and longitudes. We collected climatic conditions, soil properties, past and current fertilizer managements, and "Normal" and converted values of crop yield or N uptake. Missing values of MAT and MAP were extracted from WorldClim v2.1 (Fick & Hijmans, 2017) using latitudes and longitudes; the missing soil properties were supplemented using the Harmonized World Soil Database (HWSD v1.2 and v2.0, https://gaez.fao.org/pages/hwsd).

2.7. Statistical Analyses

All statistical analyses of microorganisms were conducted on the statistical platform R (V4.3.2). The α-diversity indices (Shannon, Inv_Simpson, Richness, and Chao1) were calculated using the "vegan" package in R (Oksanen et al., 2024), following normalization of the data to an equivalent sequencing depth via the "rrarefy" function. We standardized the value of bacterial and fungal α-diversity using the z-score (overall mean of 0 and SD of 1), and then averaged them to create an overall α-diversity of biotic community. The β-diversity of the bacterial and fungal communities were estimated based on Bray–Curtis dissimilarity between samples, and the dissimilarity was calculated using the "vegdist" function in the "vegan" package. Nonmetric multidimensional scaling (NMDS) was conducted to reflect β-diversity in both bacterial and fungal communities using the "vegan" package. An analysis of similarities [Permutational multivariate analysis of variance (PERMANOVA)] was used to determine significant differences in microbial community composition across different treatments, performed using the "anosim (adonis2)" function in the "vegan" package. Co-occurrence network analysis was based on each fertilization treatment (two straw managements with three replicates for each network). Collecting all sampling of each fertilization treatment can improve sensitivity to co-occurrence events and reveal co-occurrence patterns of soil biotic communities driven by different C and N inputs. The co-occurrence networks were constructed using the "WGCNA" package based on the Spearman correlation matrix with adjusted p values (Langfelder & Horvath, 2012). The network properties were calculated using the "igraph" package in R (Csárdi et al., 2024), and visualization was performed using Gephi software (version 0.10.1). We tested the effects of conversion impacts on the relative abundance of microbial functional groups using linear mixed-effects model in "lme4" packages (Bates et al., 2015), in which block was termed as random intercept effects. Microbial functional groups were predicted by the Functional Annotation of Prokaryotic Taxa (FAPROTAX) (Louca et al., 2016) and FungalTraits (Põlme et al., 2021) in "microeco" package and "tidyverse" and "phyloseq" packages (Liu et al., 2021; McMurdie & Holmes, 2013; Wickham et al., 2019), respectively. To link soil environmental and microbial variables to microbial communities, the correlations between soil factors and microbial diversity and functional groups were tested by "mantel.test" function in "vegan" package, and visualized by "linkET" package (Huang, 2021).

The difference in yield, straw and grain biomass, aboveground N uptake, and N surplus between treatments was considered significant at the level of $p < 0.05$ by one-way ANOVA with least significant difference method test using SPSS 25.0 (IBM Corp., Armonk, NY, USA). A paired *t*-test was used for the paired samples between the original and the conversion on yield, grain and straw biomass, grain and straw N content, aboveground (grain and straw) N uptake, N surplus, and NO_3^--N accumulation. A three-way ANOVA and a LSD's test at a 5% level of significance was used to explore the effects of N fertilizer treatment, straw management, season, and their interactive effect on yield, aboveground biomass, grain and straw N content, grain N uptake, aboveground N uptake, and N surplus. The importance analysis of resistance and recovery by "randomForest" and "rfPermute" packages in R version 4.3.2 (R Foundation for Statistical Computing, Vienna, Austria). An Structural equation model (SEM) was applied to explore the mechanisms of the direct and indirect effects of historical manure, historical N rates, conversion N rates, and other soil C and N contents on yield, aboveground N uptake, and N surplus by SPSS Amos 24.0 (IBM Corp., Armonk, NY, USA).

3. Results

3.1. Grain Production and Conversion Effect

Overall, crop production was influenced by the N application rate, straw management, and cropping season (Table S3 in Supporting Information S1). In the first year (i.e., in 2021), wheat yield ranged from 6.1 to 7.4 Mg ha^{-1} and was similar across all treatments (Figure S5a in Supporting Information S1). This was due to the increased yield in the zero N treatment following the application of manure with mineral N fertilizer (MN and MNS), and the negligible effect on crop yield of removing N applications in the high fertility treatments (Figure 1 and Figures S7, and S8 in Supporting Information S1). Compared to the original zero N (SN_0 and N_0) and optimal N (SN_{opt} and N_{opt}) treatments, the grain biomass of the manure with mineral N treatments increased by an average of 136% (178% for wheat and 93.5% for maize) and ~0%, respectively (Figure 1). The grain biomass of the zero-N (NN and NNS) treatments decreased by an average of 19.6% (13.0% for wheat and 26.2% for maize) compared to the original high-N treatments (SN_{con}, SMN_{bal}, N_{con}, and MN_{bal}). However, the maize yield of the NN treatment converted from the original SMN_{bal} treatment showed stability and remained unchanged (Figure S5b in Supporting Information S1). In contrast, other treatments converted to zero-N exhibited a significant yield decrease, with N_{con} being particularly pronounced. In the following four seasons, the above trends became increasingly divergent (Figure 1, Figures S7, and S8 in Supporting Information S1). Overall, crop yield and grain N uptake were directly and indirectly regulated by historical N (including mineral N and manure) and current-season N fertilization (Figure S11 in Supporting Information S1).

3.2. Resistance and Recovery Index for Crop Production

The resistance index of the zero-N treatments decreased over time. In the first year, there was strong yield resistance with an average resistance index of 0.94 (range from 0.90 to 0.98) for wheat and 0.86 (range from 0.81 to 0.92) for maize (Figure 2a). In the following years, the highest resistance index for yield was observed in the NN treatment converted from the original SMN_{bal} treatment (SMN_{bal}-NN), with 0.80 for wheat and 0.90 for maize in 2022, and 0.63 for wheat and 0.95 for maize in 2023. These observations indicate that the long-term addition of manure and straw results in a significant build up of a soil nutrient reserve (organic and inorganic) which results in a high yield resistance following cessation of fertilization. Overall, the NO_3^- content of the top

10.1029/2025EF007435

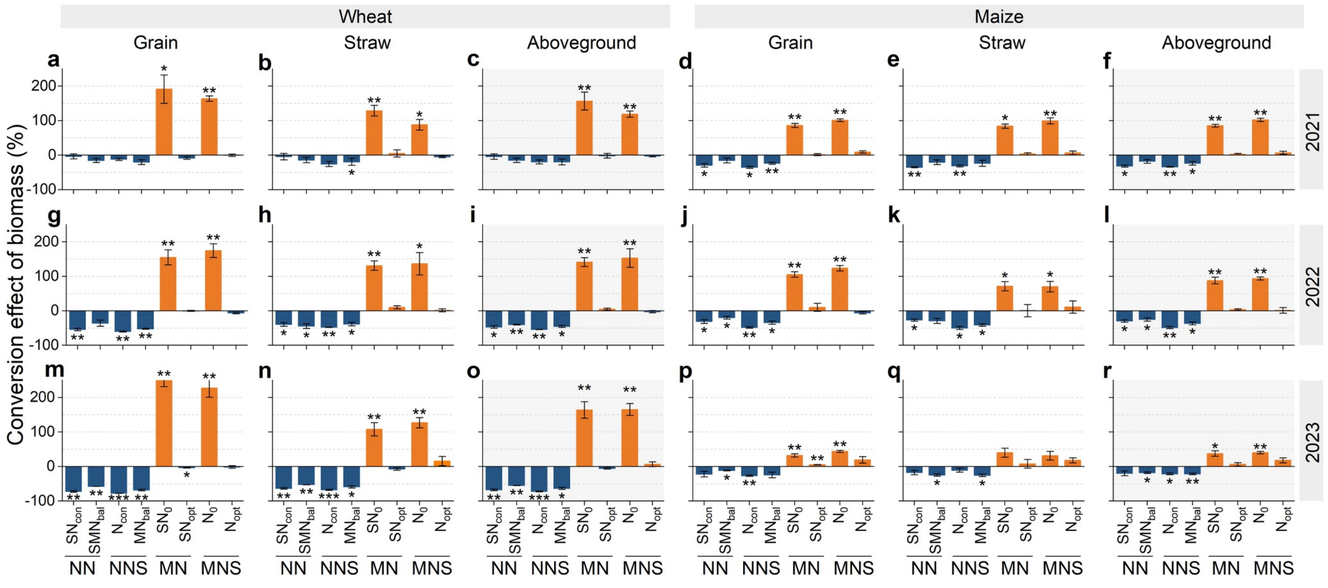

Figure 1. Conversion effect of aboveground biomass compared to the original treatments. (a–c), Wheat grain (a), straw (b), and aboveground (c) in 2021. (d–f), Maize grain (d), straw (e), and aboveground (f) in 2021. (g–i), Wheat grain (g), straw (h), and aboveground (i) in 2022. (j–l), Maize grain (j), straw (k), and aboveground (l) in 2022. (m–o), Wheat grain (m), straw (n), and aboveground (o) in 2023. (p–r), Maize grain (p), straw (q), and aboveground (r) in 2023. Year refers to the year in which the crops were harvested. ***, **, and * represent significant differences at $p < 0.001$, 0.01, and 0.05. N_0, N_{opt}, N_{con} and MN_{bal} are zero N fertilizer, optimal N, conventional N and balanced mineral N with manure treatments under the original scenario, respectively. S and M refer to straw return and cattle manure addition, respectively. NN and MN represent the non-N and manure with synthetic N treatments under the conversion scenario, respectively.

20 cm of soil, resulting from historically high N application rates, was a significant contributor to the resistance of wheat and maize, in addition to interannual differences derived from precipitation and temperature (Figure 2c).

The recovery index of the manure with mineral N treatments increased over time. In the first wheat season, the mean recovery index of yield in the (S)N_{opt}-MN(S) treatments was 0.94, which was higher than 0.89 in the (S)N_0-MN(S) treatments (Figure 2b). The mean yield recovery index for wheat was 0.96 in 2022 and 0.95 in 2023. In contrast to wheat, there was a strong and stable recovery in maize, with a mean yield recovery index of 1.00. Overall, interannual differences due to precipitation and temperature and crop type were also significant factors for yield recovery (Figure 2c). The recovery of grain N uptake also depends on historical N application rates (Figure S9c in Supporting Information S1), resulting in differences in N effects between zero N and optimal N (Table S7 in Supporting Information S1).

Maize, a C4 plant with a high photosynthetic efficiency, has a higher N uptake efficiency than wheat, a C3 plant, giving it more resistance and recovery. To assess the resistance and recovery of the whole rotation, we calculated the time variation in different years (Figure S10 in Supporting Information S1). The mean resistance indices for yield and grain N uptake in the first year were 0.90 and 0.86, respectively, and the mean recovery indices were 0.95 and 0.92, respectively. Long-term manure and straw management showed greater resistance to cessation of N application and increased prevalence over time. Past N application showed more recovery than the zero N application but changed little over time. Resistance and recovery indices of grain N uptake were lower than those of yield because crop N levels were more sensitive, usually manifesting as high yield at the expense of higher N uptake.

3.3. Global Synthesis of Resistance and Recovery

According to the analysis for the normal level (Table S2 in Supporting Information S1), a strong resistance and recovery were defined as an index greater than 0.90. The global synthesis of the median yield resistance index was 0.94, and the median recovery index was 1.00 (Figures 2c and 2d). The main reasons for high resistance were high SOC and residual soil N (Figure S13a in Supporting Information S1). To further assess the global crop productivity level after N conversion, the "potential yield" was employed as the higher yield standard to calculate the global resistance and recovery indices (Figures 2e and 2f). A comparison of the observed yield after conversion

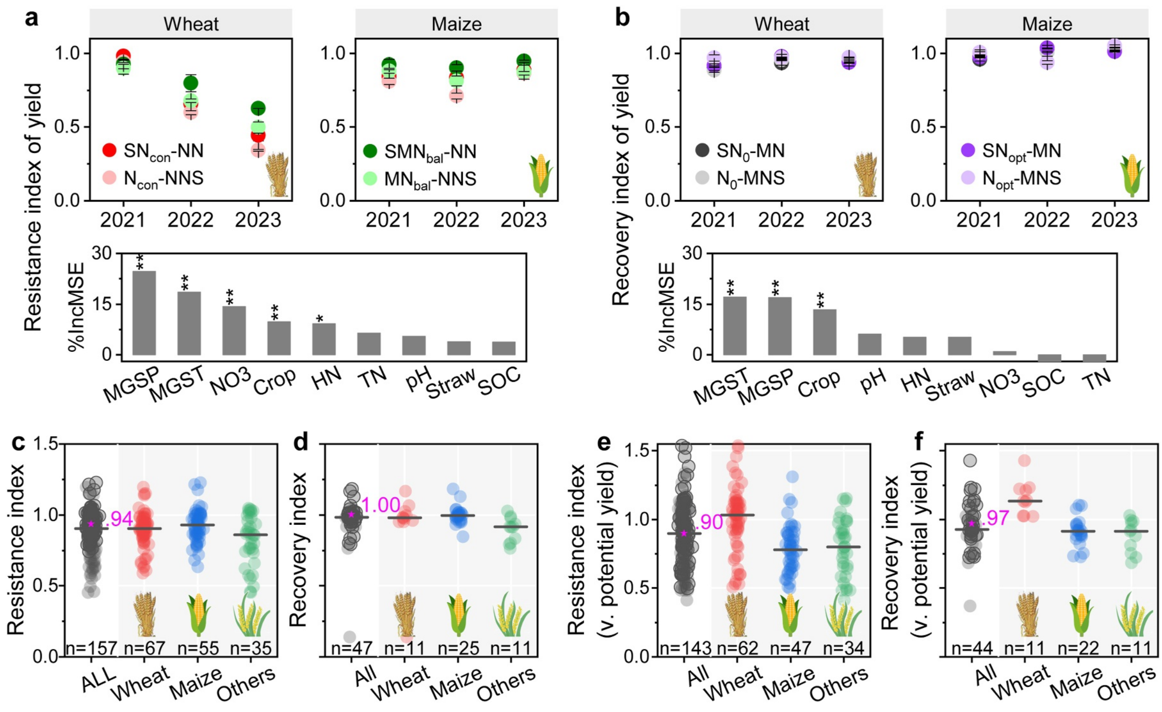

Figure 2. Resistance and recovery index of crop yield. (a), the yield resistance index of wheat and maize. (b), the yield recovery index of wheat and maize. The treatments represent "original-conversion" treatments. The relative importance (%IncMSE) of the factors were also demonstrated. (c–d), global resistance and recovery index of crop yield compared with the "Normal" yield. (e–f), global resistance and recovery index of crop yield compared with the potential yield from Mueller et al. (2012). The straight line denotes the median. The circular dots with prominent outlines on the exterior of the circle were selected based on the definitions of resistance (high fertility soil or past high N inputs) and recovery (current optimal or high N inputs), and the pink pentagram represent their median. MGSP and MGST denote mean growing season precipitation and temperature. Crop denotes the winter wheat and summer maize. HN and straw represent N fertilizer applications in historic regimes and straw return in the current year. NO_3, TN, SOC, and pH represent nitrate-N, total N, soil organic-C, and pH in the top 20 cm soil layer, respectively. ***, **, and * represent significant differences at $p < 0.001$, 0.01, and 0.05. The codes of treatments are same as Figure 1.

with the "potential yield" (Mueller et al., 2012) suggests that the resistance and recovery indexes were above 0.90. Therefore, the possibility of strong resistance and recovery is strengthened across global croplands.

3.4. Conversion Shock on N Surplus and Residual Nitrate

Residual nitrate and N surplus can be used as indicators of the environmental risks associated with the N management. N inputs (including mineral fertilizer, manure, and straw) were the key factors driving the N surplus (Figure 3b). After conversion, the highest N surplus was 173 kg N ha^{-1} yr^{-1} based on the highest N inputs of 444 kg N ha^{-1} yr^{-1} in the MNS treatments, followed by 64 kg N ha^{-1} yr^{-1} with 350 kg N ha^{-1} yr^{-1} in the MN treatments, −49 kg N ha^{-1} yr^{-1} with 69 kg N ha^{-1} yr^{-1} in the NNS treatments, and the lowest N surplus was −165 kg N ha^{-1} yr^{-1} with zero N inputs (no fertilizer, manure, and straw) in the NN treatments (Figure 3a). In the first year, the N surplus of the zero N treatments decreased by 342 kg N ha^{-1} compared to the original high N treatments (Figure S14a in Supporting Information S1). Meanwhile, the N surplus of the MN treatments increased to 134 kg N ha^{-1}. An excessive N surplus indicates a high risk of N loss to the environment, while a negative N surplus implies mining of the soil N pool, both of which are detrimental to sustainable agriculture. To account for the differences in N surplus, we compared the N surplus of the SMN balance with the N surplus of conventional double-cropping rotations in the NCP (Zhang et al., 2019). The N surplus of the SMN_{bal} and MNS treatments was comparable to the N surplus benchmark of 160 kg N ha^{-1} yr^{-1}, which was established by optimized N management as a reasonable N surplus index in Chinese double cropping systems (Zhang et al., 2019).

Compared to the original sub-plots, the soil NO_3^- pool in the converted sub-plots decreased with increasing soil depth and time, significantly reducing the risk of N loss by leaching while maintaining a suitable level for crop growth (Figures 3c and 3d). In the top 20 cm layer of soil, the NO_3^- pool decreased by 77% and 61% in the zero N treatments that had previously received conventional N and balanced mineral N with manure treatments,

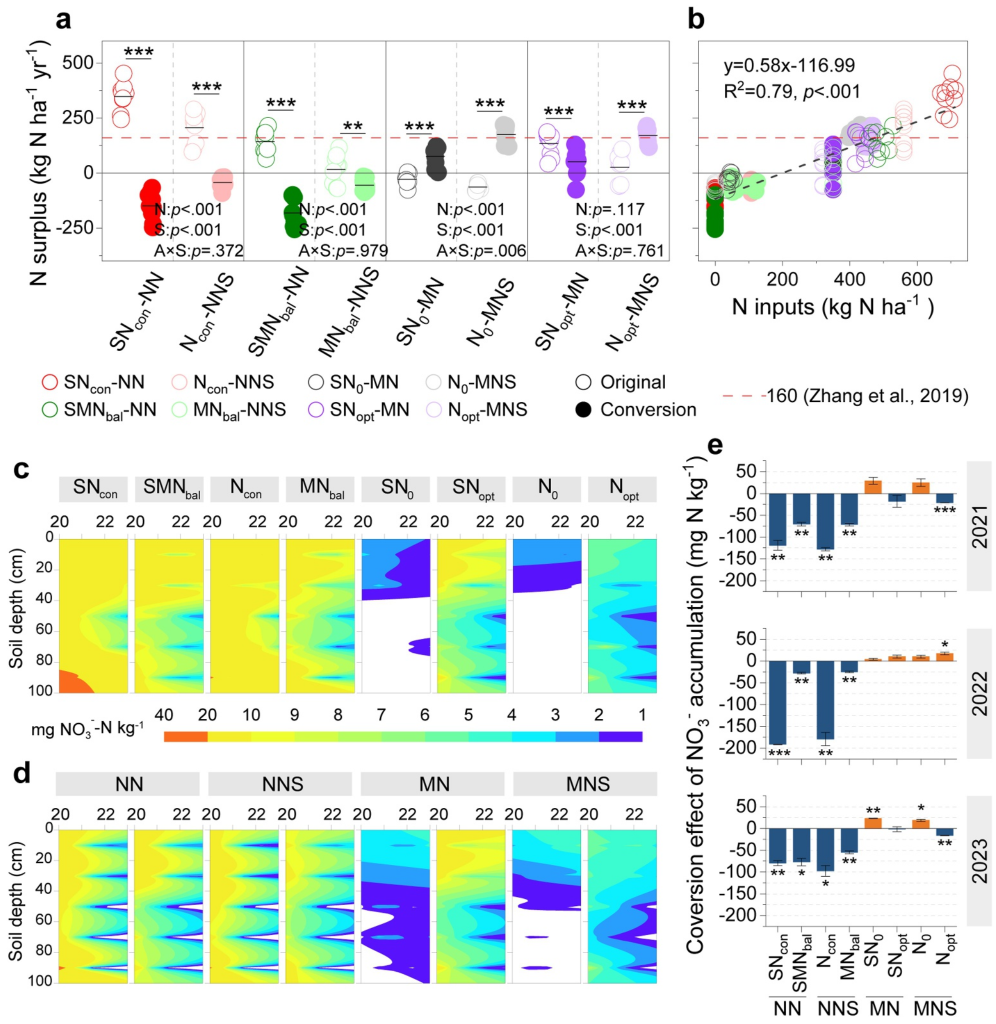

Figure 3. N surplus and spatio-temporal variation of soil nitrate N. (a), Mean N surplus during 2020–2023. The treatments represent original-conversion treatments. **, and * represent significant differences at $p < 0.01$ and 0.05. Zhang et al. (2019) suggested the N surplus benchmarks for double cropping systems at 160 kg N ha^{-1} in the North China Plain. (b), The relationship between N inputs (fertilizer, manure, and straw) and N surplus. (c), soil NO_3^- distribution in original. (d), soil NO_3^- distribution in conversion. 20 and 22 indicate the year (20−). (e), conversion effect of NO_3^- accumulation compared to the original treatments. ***, **, and * represent significant differences at $p < 0.001$, 0.01, and 0.05. The codes of treatments are same as Figure 1.

respectively. The NO_3^- pool increased by 178% in plots receiving manure with mineral N that had previously received zero N (Figure 3d). In the N fertilized plots converted from optimal N treatments, NO_3^- first decreased by 29% in 2021, then increased by 42% in 2022, and finally remained constant in 2023. This average decrease of NO_3^- accumulation in the top 1 m of soil was 81% in the zero N treatment, the increase was 136% in the manure with mineral N treatments converted from zero N treatments, and there was no change in the manure with mineral N treatments converted from optimal N treatments (Figure 3e).

3.5. Microbial Taxonomic and Functional Shocks

Long-term fertilization had a significant effect on the α-diversity of the bacterial community ($p = 0.008$; Table S6 in Supporting Information S1), whereas N conversion had no discernible effect on the α-diversity of the biotic community (Figure 4c). The α-diversity of the biotic community increased in the zero N treatments converted from the original conventional N fertilization (Figure 4c). In terms of functional composition, as classified by FAPROTAX for bacteria and Fungal Traits for fungi, cessation of N application significantly altered the

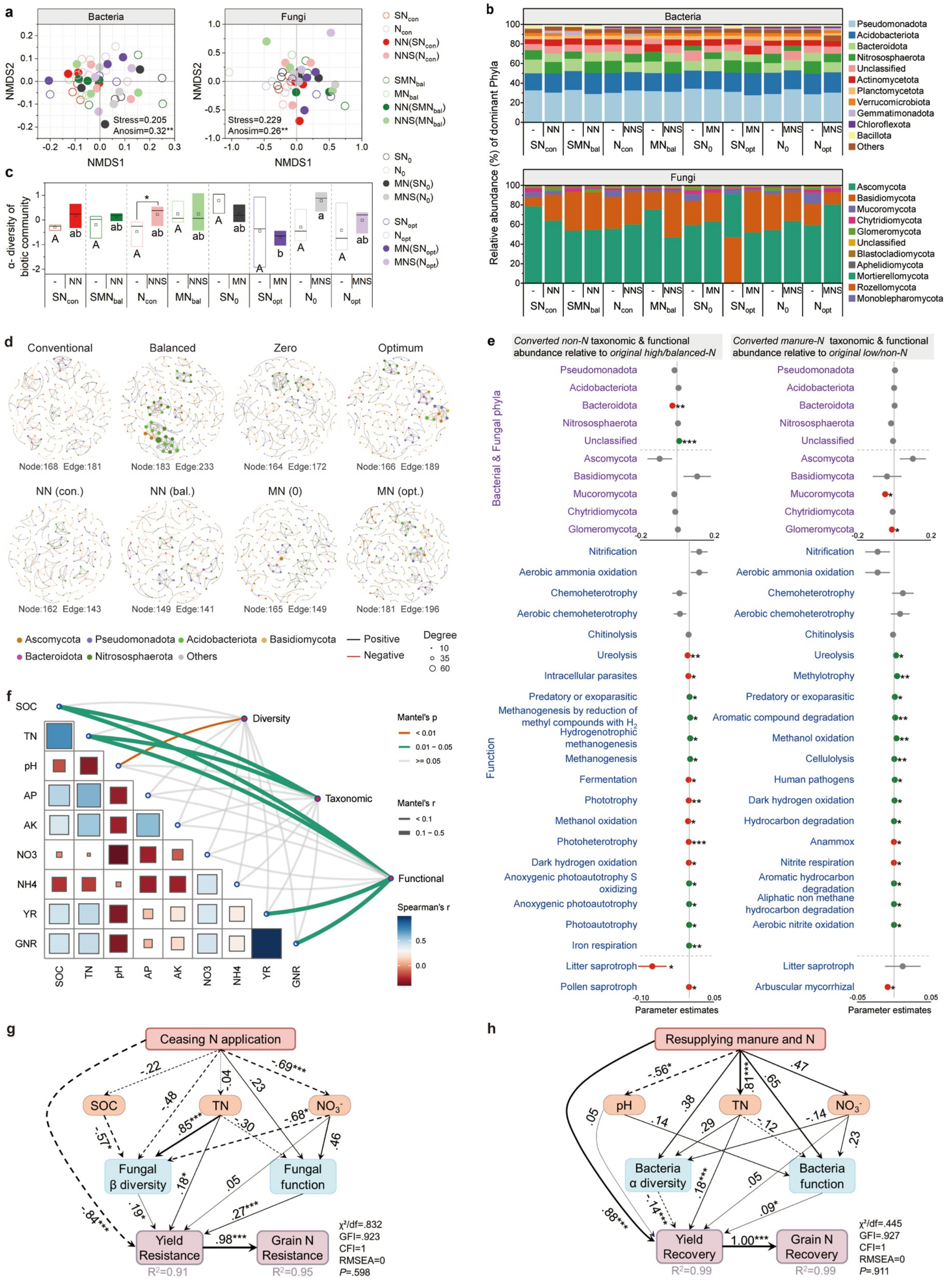

Figure 4.

abundance of some bacterial groups specialized in nutrient cycling (e.g., ureolysis, methanogenesis, phototrophy, etc.) compared with the original ecosystems (Figure 4e).

Fungal communities offset the direct negative effects of fertilizer cessation on crop yield and grain N uptake, coupled with their synergistic relationship with soil TN and NO_3^- contents, demonstrating robust support for the resistance index (Figure 4g). The reintroduction of fertilization (manure and mineral N fertilizers) also significantly increased the abundance of bacterial taxa specialized in nutrient cycling (e.g., methylotrophy, aromatic degradation and cellulolysis). The reintroduction of manure and N supplementation under N-limited conditions modulates bacterial diversity and functional profiles through the mediation of key edaphic parameters (soil pH, TN, and NO_3^-), which serves as a critical determinant for the recovery of crop productivity (Figure 4h). This clearly demonstrates that microbial functional redundancy in soil-crop systems significantly modulates ecosystem stability metrics, in particular enhancing resistance and recovery indices under N perturbation stress (Figures 4e–4h).

4. Discussion

Our study provides evidence for an asynchrony in crop responses to N addition or removal with strong resistance of soils that had received long-term N applications, and in contrast the extremely rapid strong recovery of long-term N depleted soils (Figures 2 and 5). We found that cessation of N supply in the first year maintained high crop production and soil microbial diversity in soils that had received long-term high N applications due to NO_3^- retention, while reducing the high N surplus to a low level. The long-term N depleted soils showed high crop production, while the N surplus increased to a reasonable level when N fertilizer was reapplied. Alternating cessation and reapplication of fertilizer in successive cropping seasons could maintain high crop yields while balancing the risk of N loss and the depletion of the soil N pool. An important prerequisite is that the soil must contain adequate levels of other important macro- and micro-nutrients, such as phosphorus and potassium, for crops to reach their full potential (Burke et al., 2017; van der Velde et al., 2014). Optimal crop management also involves the integrated use of knowledge-based N management practices, including split fertilization, deep placement applications, reduced tillage, and other agronomic techniques.

4.1. Strong Resistance Helps Develop Sustainable Agriculture

We observed a strong resistance to yield changes in the high fertility soils during the first year, resulting in reduced soil NO_3^- and N surplus (Figure 5). Strong resistance was defined as maintaining the high production levels of wheat and maize in the region when compared to the zero N application. Yield resistance in the first year was well above the lower limit of the region's normal yield and is consistent with China's projected yield requirements by 2030 (Figure 5b and Table S2 in Supporting Information S1). Better yields were achieved by reducing or even stopping N inputs in some areas (Ahvo et al., 2023). This was due to soil NO_3^- retention and accumulated high N surplus (or narrow C:N ratio) in soil organic fractions (Figures S10 and S13a in Supporting Information S1), providing sufficient N for high crop production for several cropping seasons (Sebilo et al., 2013). Microbial functional disarray reflects a community adapted to high, readily available N inputs struggling to rewire its metabolism (Isbell et al., 2013). The increase in α diversity of the biological community when ceasing N reflects the release of microbial diversity from N enrichment (K. Li et al., 2025a). However, soil microbial diversity and function showed a delayed response cessation or reapplication of fertilizer N (Figure 4 and Table S6 in Supporting Information S1), as the dynamics of microbial communities are mainly influenced by soil metal ions, pH, and the plant community rather than N availability (Chen et al., 2024; Rousk et al., 2010;

Figure 4. Effects of N conversion on different microbial taxa compared with original and environmental drivers of microbial composition. (a), NMDS analyses of Bray–Curtis distances showing dissimilarities among taxonomic composition between converted and original treatments. (b), Relative abundance of dominant Phyla. (c), Biotic α-diversity. (d), Co-occurrence network patterns and network stability of biotic community under different treatments. (e), Effect sizes of converting impacts on the relative abundance of microbial taxonomic and functional groups as classified by FAPROTAX (bacteria) and FungalTraits (fungal) compared with original. The estimated effect sizes are regression coefficients based on the linear mixed-effects models. Data are presented as mean ± s.e.m. of the estimated effect sizes. Non-significant changes are denoted by gray dots. (f), Pairwise comparisons of environmental factors are shown, with a color gradient denoting Spearman's correlation coefficients. Edge width corresponds to Mantel's r statistic for the corresponding distance correlations, and edge color denotes the statistical significance based on 9999 permutations. YR and GNR represent yield and grain N uptake resistance or recovery. (g–h), Structural equation models showing the relationships among N conversion impacts, soil variables, microbial diversity and functional composition. Solid and dashed arrows indicate positive and negative relationships, respectively. Numbers near the pathway arrow indicate the standard path coefficients. ***, **, and * indicate significant relationships at $p < 0.001$, 0.01, and 0.05. R^2 represents the proportion of variance explained for every dependent variable.

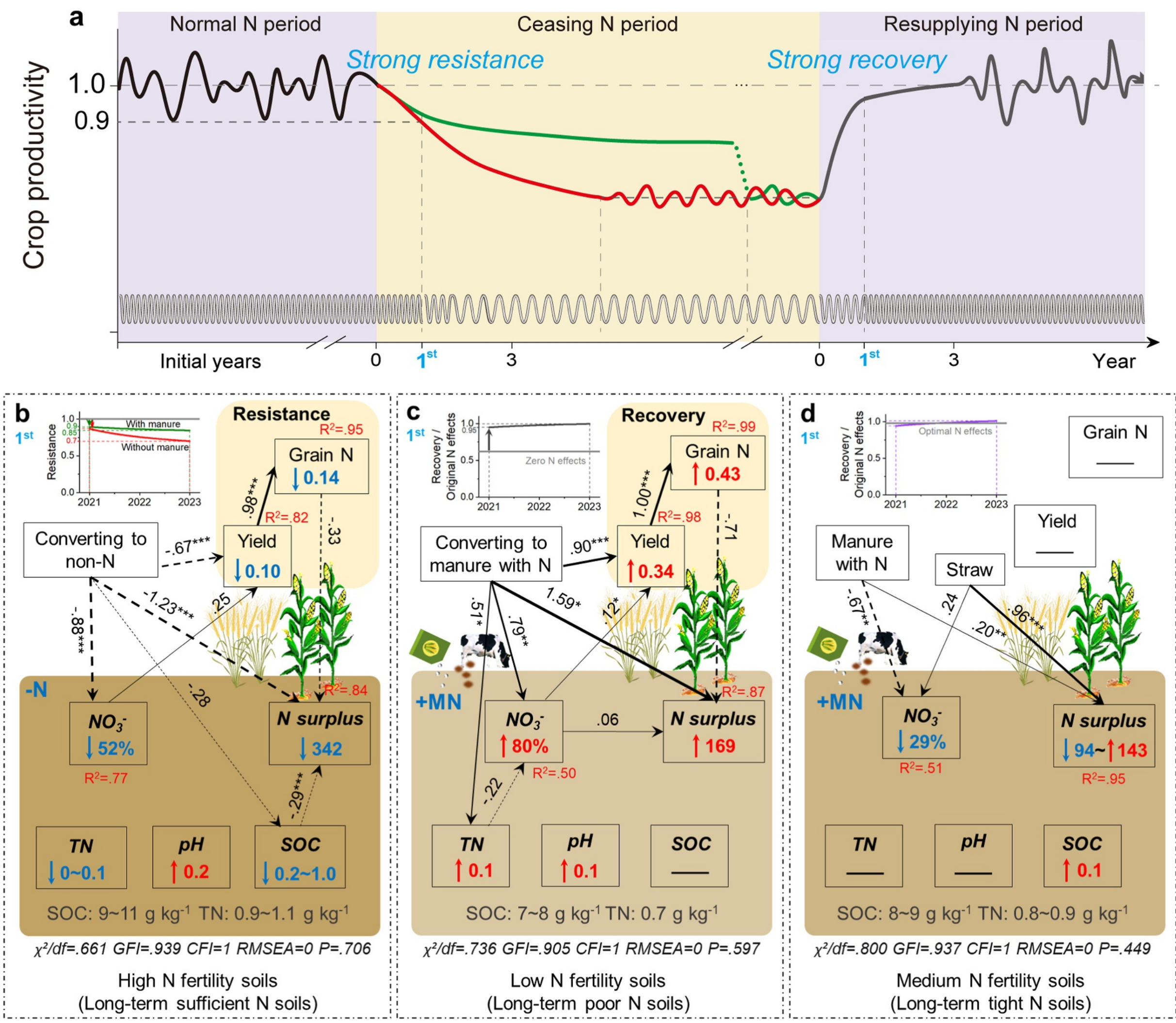

Figure 5. The resistance and recovery of crop productivity from contrasted soil fertility. (a), Schematic illustration of resistance and recovery index. (b), the change of resistance index in the first year. (c), the change of recovery index from the original zero N scenario in the first year. (d), crop production from the original optimal N scenario in the first year.

Stefanowicz et al., 2008). Rather than attributing the actual high yield in this region to a significant reduction in N inputs, this suggests that high yields could be achieved with lower N inputs in similar areas due to the abundant residual N available to crops (Ahvo et al., 2023). It is evident that the environmental risks, including the high N surplus and NO_3^- residues, have been mitigated by the cessation of N fertilization (Figure 5b), and the change of cropping seasons with no and balanced N fertilization allows to achieve a balance between high yield and low environmental impact in high input regions.

We also found that the largest decreases in yield resistance were for synthetic N fertilizer alone, while added manure and returned straw tended to be less negatively affected by the cessation of N fertilization (Figures S10 and S13a in Supporting Information S1). The higher yield resistance of the high synthetic N inputs alone is likely to be more dependent on agronomic N inputs than the combination of manure with mineral N fertilizer and the variation in high yield resistance is more easily explained by synthetic N rates. This finding confirms results from a previous study that predicted yield changes in response to changes in N inputs, where higher yield was also most influenced by agricultural input use (Ahvo et al., 2023). Manure management to replace mineral fertilizers significantly stimulated overall soil NO_3^- retention, microbial interactions and soil quality improvement (e.g., SOC and TN etc.) ultimately maintaining crop yields, while reducing N surplus (Figures 3–5, and Figure S15, and Table S1 in Supporting Information S1). Sufficient available C and N in organic C-rich soils also increases the assimilates for soil microorganisms to sustain growth, which promotes N turnover and helps to achieve a target yield (Luo et al., 2023; Neal et al., 2022) and explains the stronger yield resistance.

A critical question raised by our findings is the origin of the soil NO_3^- that sustained crop productivity after N cessation. While we cannot definitively partition NO_3^- derived from direct residual fertilizer versus that from mineralization of organic N without isotopic tracers, several lines of evidence strongly point to the farmer as the dominant pathway. First, the significant positive correlation between resistance and NO_3^- levels by site experiments and global research analysis in the first year of N cessation (Figure 5b and Figure S13a in Supporting Information S1). Second, the temporal pattern—strong resistance (i.e., maintained high yield) in a single-season/year pulse rather than multiple seasons—is inconsistent with the slow, continuous release from organic matter but aligns with the depletion of a finite residual fertilizer NO_3^- pool. However, the mineralization of organic N accumulated historically has always been one of the important sources of N to crop (Yan et al., 2020). Fertilizer-derived organic N has a long residence time, with a slow release of N over period of 28 years (Sebilo et al., 2013; Zhao et al., 2024). Therefore, we believe that NO_3^- from historical fertilizer residues and organic N mineralization jointly supported the strong resistance for crop production in the first year, despite the lack of directly evidence.

4.2. Strong Recovery Dedicated to Agricultural Production Recovery

The immediate crop production and environmental benefits of N fertilizer resupply are striking, especially when combined with manure replenishment and optimal management practices (Figures 5a–5c and Figure S13b in Supporting Information S1), which is consistent with our previous studies (Tian et al., 2023; Zhang et al., 2021). Strong recovery was defined as the restoration of high production for cereal crops in the region following N fertilizer reapplication. The yield recovery far exceeded the lower limit of normal yield in the region and China's yield requirement for self-sufficiency by 2030 (Figure 5c and Table S2 in Supporting Information S1). This phenomenon can be attributed to the addition of N fertilizer following a previous crop season with zero N application (Figure 5c), which enhances both the dominant microbial taxa and the interactions between microorganisms (Figure 4). This is increase in microbiome interactions was likely promoted by incrieasing C and N availability in a soil with no other discernible soil quality problem (Tian et al., 2023; Wang et al., 2023; Q. Xu et al., 2024). The increase in the microbial functional potential of nutrient cycling provides a mechanistic framework to interpret the observed crop recovery pattern (Li et al., 2023). This suggests a rapid activation of microbial communities, which are geared toward mineralizing previously inaccessible soil organic matter and likely releasing both C and N locked in complex compounds. This effect transiently enhances soil N availability, facilitating vigorous crop N uptake following re-supplying N (Chen et al., 2024). We also found that optimization consistently increased the N surplus to a benchmark that balances soil supply and crop uptake (Zhang et al., 2019), while reducing N losses and increasing crop N uptake. This highlights the importance of combining N fertilizer and agronomic optimization management strategies to improve crop production and reduce environmental costs (Elrys et al., 2023). In general, the long-term zero N regime soils demonstrated remarkable recovery due to the absence of limiting factors that impede crop production, including agronomic management, soil nutrients, and soil properties.

The recovery of crop production on zero and optimal N soils was dramatically different as a result of the different historical N management regimes, despite the identical source, rate, time, and location of N fertilizer application in the conversion scenario (Figures 2 and 5, Figures S9, and S10 in Supporting Information S1). The crop production of the optimal N regime remained at a constant level, while the soil of the previously zero N regime showed a strong recovery after the reapplication of N fertilization (Figures 5c and 5d). This was not surprising, as optimizing fertilization methods is a knowledge-based and efficient management approach that has a positive impact on sustainable agriculture (Elrys et al., 2023; Xiao et al., 2024; Yin et al., 2021).

4.3. Multidimensional Microbial Responses and Limitations

The distinct functional reorganization in response to N cessation versus re-addition elucidates the specific microbial strategies underpinning ecosystem resistance and recovery (Allison & Martiny, 2008). Following the cessation of long-term N fertilization, the decline in functions tied to readily available N (e.g., ureolysis) and simple C fermentation reflects a downregulation of pathways dependent on high resource quality. Concurrently, the significant increase in methanogenesis by multiple pathways, iron respiration, and diverse photoautotrophy signifies a profound metabolic shift. The microbial community was forced to utilize alternative, less energetically favorable electron acceptors and energy sources, indicating a stress response toward resource conservation and survival metabolism (Chen et al., 2024; Fierer et al., 2012; Yan et al., 2025). Crucially, this functionally "disrupted" state does not collapse crop productivity because the legacy of SOC and residual NO_3^- provides a direct, buffering pool of resources for crops. The high resistance is thus maintained not by microbial functional efficiency, but by the abiotic buffering of historical nutrient capital, allowing crops to bypass temporary microbial metabolic inefficiency. In contrast, N re-addition to historically depleted-N soils triggered a rapid, coordinated upregulation of functions geared toward exploiting complex organic matter: methylotrophy, aromatic compound degradation, cellulolysis, and hydrocarbon degradation. The co-increase in aerobic nitrite oxidation further points to enhanced nitrification, boosting crop-available NO_3^-. The decline in arbuscular mycorrhizal symbiosis suggests a strategic reallocation by the crop away from cost-intensive symbiotic nutrient foraging, as N is now readily available. This functional reprogramming depicts a community switching to an acquisitive, high-activity strategy, which rapidly mineralizes both old soil organic matter and new fertilizer inputs, thereby flooding the soil with available nutrients to drive the observed rapid crop recovery and high N uptake (R. Chen et al., 2014; X. Chen et al., 2014; L. Li et al., 2025; Q. Xu et al., 2024). These responses may also be influenced by soil characteristics not fully captured by N treatments alone, such as pH, soil organic matter quality, and microaggregate structure, which act as environmental filters selecting for distinct functional traits (Wang et al., 2023; Yang et al., 2022). This suggests that inherent soil properties interact with historical management to shape the functional trajectory and stability of microbial communities (Philippot et al., 2024; Rahmati et al., 2023).

Our integrated analysis reveals a nuanced picture of microbial responses to N conversion. The absence of a significant net shift in aggregated microbial indices (e.g., overall functional) in response to N conversion by the SEM likely reflects functional compensation and reorganization within the community (Figures 4g and 4h). Specifically, the enhancement of certain bacterial processes (e.g., methylotrophy and aromatic degradation) concurrent with the attenuation of specific fungal functions (e.g., arbuscular mycorrhizal) suggests a reconfiguration of metabolic priorities rather than a wholesale community change. Crucially, however, the SEM robustly confirmed that the resulting microbial state is a significant mediator of crop productivity. This emphasizes that the functional configuration and specific traits of the microbiome, rather than its gross microbial biomass or diversity per se, are the key mechanistic links between N management and crop production (Bardgett & van der Putten, 2014).

We concurrently acknowledge the inherent limitations of the SEM framework applied here. While SEM powerfully evaluates the consistency of our a priori hypothetical structure with observational data, it cannot independently establish causality. The model's validity is contingent upon the variables included, and unmeasured biotic or abiotic factors may influence the proposed relationships. Furthermore, our static model captures relationships at a fixed point in time and may not reflect the dynamics of these interactions during the transition between disturbance and recovery phases. These considerations do not undermine the supported pathways but appropriately bound their interpretation. Future manipulative experiments and temporal series analyses are warranted to dynamically validate these mechanistic inferences.

4.4. Implications and Uncertainties

Agricultural N management not only produces immediate agronomic effects, but also leaves a profound legacy of biogeochemicals that continues to affect the functional properties of the system. Our study demonstrates that historical N regimes (including historical N rates and soil NO_3^- residues) are a key driving factor of strong resistance in agricultural systems, as evidenced by both single-site experiments and global research analysis (Figure 5 and Figure S13 in Supporting Information S1). This cross-scale validation confirms that the mechanism uncovered at the process-oriented site represents a generalizable driver, providing a unifying mechanistic framework for understanding and managing agricultural ecosystem resilience worldwide. While specific manifestations of this mechanism, such as dominant microbial communities and crop uptake efficiency, may be influenced by local environmental factors, the overarching causal pathway indicates that management history constrains system resilience by altering soil biotic and abiotic properties (Ahvo et al., 2023; Sebilo et al., 2013). Consequently, our findings suggest that future strategies for bolstering global agricultural resilience should prioritize both current and historical fertilization managements.

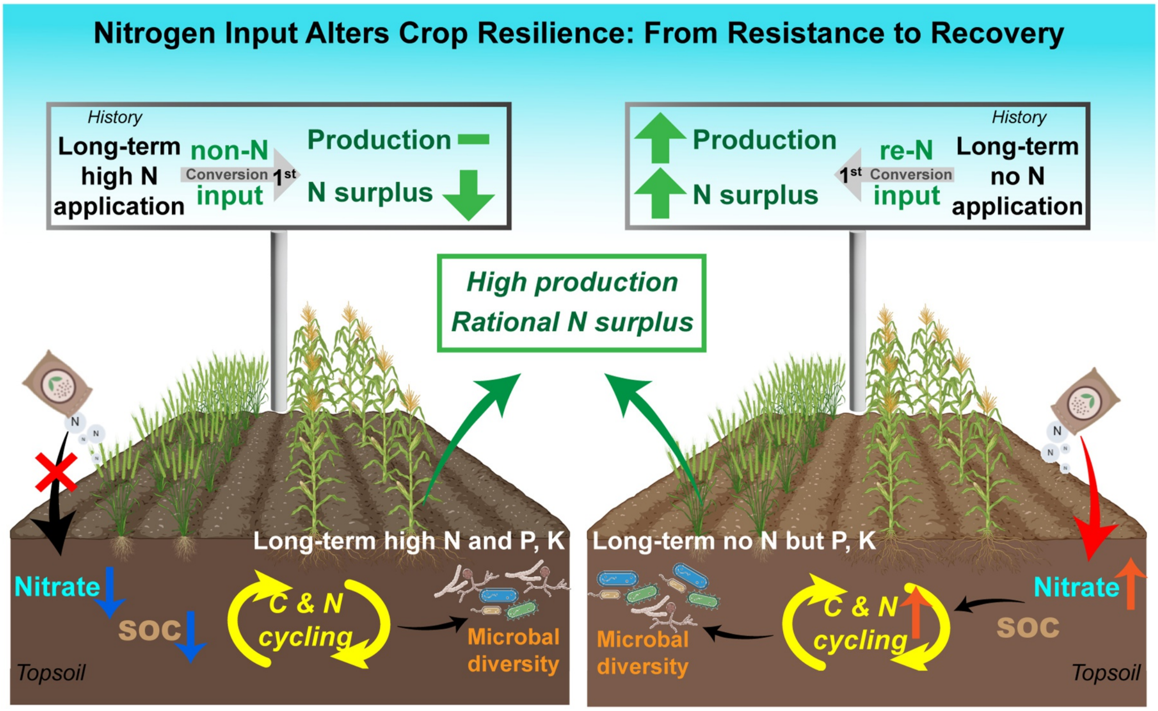

Figure 6. Schematic illustration of system integration from issues to outcomes.

Empowering local agriculture to achieve greater productivity and environmental performance though site-specific best management practices is critical as we strive for a more equitable and sustainable future. Production patterns vary around the world. e.g., countries with a high population demand for food (i.e., India and China) tend to over-fertilize as "insurance" against crop yield losses (Ju et al., 2009). This has led to large N accumulation in soils and dramatic environmental pollution, even though high production has been achieved (Ladha et al., 2020). The other locations with lower agricultural inputs (e.g., sub-Saharan Africa) results in low yield, and a vicious downward cycle driven by the mining of precious soil N stocks (Mueller et al., 2012). Both "too much" and "too little" N fertilizer inputs coexist in current global agriculture, so best management practices are targeted to specific sites based on local agricultural conditions (Gu et al., 2023). Therefore, we propose the concept of "strong resistance" to temporarily cease (or reduce) N applications where excessive N applications are occurring to minimize environmental risks at local and national levels while maintaining high crop productivity (Figure 6). In addition, the findings of "strong recovery" have inspired strong confidence in the potential to bolster agricultural productivity in regions with impoverished and underdeveloped agriculture. This can be achieved by restoring marginal land to productive farmland, thereby fostering agricultural resilience. It is precisely in such operational contexts that the demonstrated resilience of agro-ecosystems (encompassing both resistance and recovery capacities) underpins the central role of such adaptive capacities in building confidence for advancing quality-assured sustainable agricultural intensification.

While the soil NO_3^- accumulation and N surplus inherently imply the risk of N losses, there are some uncertainties. The improvement of agricultural management has great potential to enhance N use efficacy by crop and mitigate soil N loss (Wang et al., 2024; Zhang et al., 2015). In the regions with low N input, increasing N input has the potential to increase food production, especially in Africa (Gu et al., 2023). However, temperature was an important variable for high ammonia volatilization in African soils (P. Xu et al., 2024). With high ammonia volatilization in this region, it is necessary to enhance management practices (e.g., 4R nutrient stewardship including enhanced-efficiency fertilizers and organic amendments) to reduce N losses (Gu et al., 2023). Furthermore, the rate and stability of N immobilization into soil organic matter will critically influence whether added N is temporarily sequestered or becomes susceptible to future loss (Ling et al., 2025). Consequently, the proposed crop resilience (resistance and recovery) strategy should be viewed as a core framework that necessitates integration with site-specific best management practices, rather than a universal and simplistic conclusion.

5. Conclusions

This study provides an insight into sustainable food production practices, emphasizing the significance of flexible management in specific regions (long-term over-fertilized or high-fertility soils vs. long-term N-deficient soils) for food security and environmental sustainability. In low-fertility soils with deficient N globally, if no other limitations prevail, resupplying N can rapidly enhance yields and address the prevailing food crisis. Conversely, a reduced N application in high-fertility (high residual N) soils still can sustain high yields with less N losses, thereby minimizing environmental risks. These conversion effects can be explained by stimulated soil microbial activity and promoted soil nutrient turnover. Furthermore, a global literature on agricultural crop production resistance and recovery underscores the resilience of crop productivity.

Conflict of Interest

The authors declare no conflicts of interest relevant to this study.

Availability Statement

The raw reads from Illumina sequencing have been deposited at NCBI (https://www.ncbi.nlm.nih.gov/sra) under the accession no. SRR33932391-33932438 (16S) and SRR33944823-33944870 (ITS). All data needed to evaluate the conclusions in the paper are present in the paper and/or the Supporting Information S1. The data on which this article is based, including the Data Set S1, are available in Tian (2025).

Acknowledgments

This work was supported by the National Natural Science Foundation of China (Grant. U24A20625 and 12411530100), and Hainan University Startup Fund (Grant KYQD(ZR)-20098 and KYQD(ZR)-21028). We thank Qi Li, Guannan Wang, and Na Song for helpful works in sampling and determination at Shangzhuang Experimental Station from October 2020 to June 2022.

References

Ahvo, A., Heino, M., Sandström, V., Chrisendo, D., Jalava, M., & Kummu, M. (2023). Agricultural input shocks affect crop yields more in the high-yielding areas of the world. *Nature Food*, *4*(12), 1037–1046. https://doi.org/10.1038/s43016-023-00873-z

Allison, S. D., & Martiny, J. B. H. (2008). Resistance, resilience, and redundancy in microbial communities. *Proceedings of the National Academy of Sciences of the United States of America*, *105*(supplement_1), 11512–11519. https://doi.org/10.1073/pnas.0801925105

Bardgett, R., & van der Putten, W. (2014). Belowground biodiversity and ecosystem functioning. *Nature*, *515*(7528), 505–511. https://doi.org/10.1038/nature13855

Bates, D., Mächler, M., Bolker, B., & Walker, S. (2015). Fitting linear mixed-effects models using lme4. *Journal of Statistical Software*, *67*, 1–48. https://doi.org/10.18637/jss.v067.i01

Battye, W., Aneja, V. P., & Schlesinger, W. H. (2017). Is nitrogen the next carbon? *Earth's Future*, *5*(9), 894–904. https://doi.org/10.1002/2017ef000592

Bodirsky, B. L., Popp, A., Lotze-Campen, H., Dietrich, J. P., Rolinski, S., Weindl, I., et al. (2014). Reactive nitrogen requirements to feed the world in 2050 and potential to mitigate nitrogen pollution. *Nature Communications*, *5*(1), 3858. https://doi.org/10.1038/ncomms4858

Bouwman, L., Goldewijk, K. K., Van Der Hoek, K. W., Beusen, A. H. W., Van Vuuren, D. P., Willems, J., et al. (2013). Exploring global changes in nitrogen and phosphorus cycles in agriculture induced by livestock production over the 1900-2050 period. *Proceedings of the National Academy of Sciences*, *110*(52), 20882–20887. https://doi.org/10.1073/pnas.1012878108

Burke, W. J., Jayne, T. S., & Black, J. R. (2017). Factors explaining the low and variable profitability of fertilizer application to maize in Zambia. *Agricultural Economics*, *48*(1), 115–126. https://doi.org/10.1111/agec.12299

Chaer, G., Fernandes, M., Myrold, D., & Bottomley, P. (2009). Comparative resistance and resilience of soil microbial communities and enzyme activities in adjacent native forest and agricultural soils. *Microbial Ecology*, *58*(2), 414–424. https://doi.org/10.1007/s00248-009-9508-x

Chen, M., Zheng, Y., Zhai, X., Ma, F., Chen, J., Stevens, C., et al. (2024). Metal ions steer the duality in microbial community recovery from nitrogen enrichment by shaping functional groups. *Global Change Biology*, *30*(8), e17475. https://doi.org/10.1111/gcb.17475

Chen, R., Senbayram, M., Blagodatsky, S., Myachina, O., Dittert, K., Lin, X., et al. (2014). Soil C and N availability determine the priming effect: Microbial N mining and stoichiometric decomposition theories. *Global Change Biology*, *20*(7), 2356–2367. https://doi.org/10.1111/gcb.12475

Chen, X., Cui, Z., Fan, M., Vitousek, P., Zhao, M., Ma, W., et al. (2014). Producing more grain with lower environmental costs. *Nature*, *514*(7523), 486–489. https://doi.org/10.1038/nature13609

Csárdi, G., Nepusz, T., Traag, V., Horvát, S., Zanini, F., Noom, D., et al. (2024). Igraph: Network analysis and visualization in r. *R package version 2.0.3*. https://doi.org/10.5281/zenodo.7682609

Edgar, R. C. (2013). Uparse: Highly accurate otu sequences from microbial amplicon reads. *Nature Methods*, *10*, 996–998. https://doi.org/10.1038/nmeth.2604

Elrys, A. S., Wang, J., Meng, L., Zhu, Q., El-Sawy, M. M., Chen, Z., et al. (2023). Integrative knowledge-based nitrogen management practices can provide positive effects on ecosystem nitrogen retention. *Nature Food*, *4*(12), 1075–1089. https://doi.org/10.1038/s43016-023-00888-6

Erisman, J. W., Sutton, M. A., Galloway, J., Klimont, Z., & Winiwarter, W. (2008). How a century of ammonia synthesis changed the world. *Nature Geoscience*, *1*(10), 636–639. https://doi.org/10.1038/ngeo325

FAO, IFAD, UNICEF, WFP, & WHO. (2024). *The state of food security and nutrition in the world 2024 – Financing to end hunger, food insecurity and malnutrition in all its forms*. FAO. https://doi.org/10.4060/cd1254en

Feng, K., Zhang, Z., Cai, W., Liu, W., Xu, M., Yin, H., et al. (2017). Biodiversity and species competition regulate the resilience of microbial biofilm community. *Molecular Ecology*, *26*(21), 6170–6182. https://doi.org/10.1111/mec.14356

Fick, S. E., & Hijmans, R. J. (2017). Worldclim 2: New 1-km spatial resolution climate surfaces for global land areas. *International Journal of Climatology*, *37*(12), 4302–4315. https://doi.org/10.1002/joc.5086

Fierer, N., Lauber, C., Ramirez, K., Zaneveld, J., Bradford, M. A., & Knight, R. (2012). Comparative metagenomic, phylogenetic and physiological analyses of soil microbial communities across nitrogen gradients. *ISME J*, *6*(5), 1007–1017. https://doi.org/10.1038/ismej.2011.159

Foley, J. A., Ramankutty, N., Brauman, K. A., Cassidy, E. S., Gerber, J. S., Johnston, M., et al. (2011). Solutions for a cultivated planet. *Nature*, *478*(7369), 337–342. https://doi.org/10.1038/nature10452

Gu, B., Zhang, X., Lam, S. K., Yu, Y., van Grinsven, H. J. M., Zhang, S., et al. (2023). Cost-effective mitigation of nitrogen pollution from global croplands. *Nature*, *613*(7942), 77–84. https://doi.org/10.1038/s41586-022-05481-8

Hasegawa, T., Sakurai, G., Fujimori, S., Takahashi, K., Hijioka, Y., & Masui, T. (2021). Extreme climate events increase risk of global food insecurity and adaptation needs. *Nature Food*, *2*(8), 587–595. https://doi.org/10.1038/s43016-021-00335-4

Huang, H. (2021). Linket: Everything is linkable. *R package version 0.0.7.4*. https://github.com/Hy4m/linkET

Isbell, F., Tilman, D., Polasky, S., Binder, S., & Hawthorne, P. (2013). Low biodiversity state persists two decades after cessation of nutrient enrichment. *Ecology Letters*, *16*(4), 454–460. https://doi.org/10.1111/ele.12066

Ju, X. T., Xing, G. X., Chen, X. P., Zhang, S. L., Zhang, L. J., Liu, X. J., et al. (2009). Reducing environmental risk by improving n management in intensive Chinese agricultural systems. *Proceedings of the National Academy of Sciences*, *106*(9), 3041–3046. https://doi.org/10.1073/pnas.0813417106

Kaufman, L. H. (1982). Stream aufwuchs accumulation: Disturbance frequency and stress resistance and resilience. *Oecologia*, *52*(1), 57–63. https://doi.org/10.1007/BF00349012

Ladha, J. K., Jat, M. L., Stirling, C. M., Chakraborty, D., Pradhan, P., Krupnik, T. J., et al. (2020). Achieving the sustainable development goals in agriculture: The crucial role of nitrogen in cereal-based systems. In D. L. Sparks (Ed.), *Adv. Agron* (pp. 39–116). Academic Press. https://doi.org/10.1016/bs.agron.2020.05.006

Langfelder, P., & Horvath, S. (2012). Fast r functions for robust correlations and hierarchical clustering. *Journal of Statistical Software*, *46*(11), 1–17. https://doi.org/10.18637/jss.v046.i11

Li, K., Wang, J., Zhou, Z., Wu, J., Bo, X., Shen, M., & Zou, J. (2025). Nitrogen enrichment reverses microbial biomass-function relationships over time in a global meta-analysis. *Global Change Biology*, *31*(9), e70514. https://doi.org/10.1111/gcb.70514

Li, L., Xue, C., Wang, Y., Liu, M., Guo, J., Liu, M., et al. (2025). Microbial lifestyles adapted to distinct soil fertility. *Soil Biol. Biochem.*, *212*, 110023. https://doi.org/10.1016/j.soilbio.2025.110023

Li, R., Ren, C., Wu, L., Zhang, X., Mao, X., Fan, Z., et al. (2023). Fertilizing-induced alterations of microbial functional profiles in soil nitrogen cycling closely associate with crop yield. *Environmental Research*, *231*, 116194. https://doi.org/10.1016/j.envres.2023.116194

Ling, J., Dungait, J. A. J., Delgado-Baquerizo, M., Cui, Z., Zhou, R., Zhang, W., et al. (2025). Soil organic carbon thresholds control fertilizer effects on carbon accrual in croplands worldwide. *Nature Communications*, *16*(1), 3009. https://doi.org/10.1038/s41467-025-57981-6

Liu, C., Cui, Y., Li, X., & Yao, M. (2021). Microeco: An r package for data mining in microbial community ecology. *FEMS Microbiology Ecology*, *97*(2), fiaa255. https://doi.org/10.1093/femsec/fiaa255

Liu, J., Li, J., Ma, Y., Wang, E., Liang, Q., Jia, Y., et al. (2019). Crop productivity and nitrogen balance as influenced by nitrogen deposition and fertilizer application in north China. *Sustainability*, *11*(5), 1347. https://doi.org/10.3390/su11051347

Louca, S., Parfrey, L. W., & Doebeli, M. (2016). Decoupling function and taxonomy in the global ocean microbiome. *Science*, *353*(6305), 1272–1277. https://doi.org/10.1126/science.aaf4507

Luo, N., Meng, Q., Feng, P., Qu, Z., Yu, Y., Liu, D. L., et al. (2023). China can be self-sufficient in maize production by 2030 with optimal crop management. *Nature Communications*, *14*(1), 2637. https://doi.org/10.1038/s41467-023-38355-2

McMurdie, P. J., & Holmes, S. (2013). Phyloseq: An r package for reproducible interactive analysis and graphics of microbiome census data. *PLoS One*, *8*(4), e61217. https://doi.org/10.1371/journal.pone.0061217

Mueller, N. D., Gerber, J. S., Johnston, M., Ray, D. K., Ramankutty, N., & Foley, J. A. (2012). Closing yield gaps through nutrient and water management. *Nature*, *490*(7419), 254–257. https://doi.org/10.1038/nature11420

NBSC. (2023). *China statistical yearbook*. China Statistics Press. Retrieved from https://www.stats.gov.cn/sj/ndsj/2023/indexeh.htm

Neal, A. L., Barrat, H. A., Bacq-Lebreuil, A., Qin, Y., Zhang, X., Takahashi, T., et al. (2022). Arable soil nitrogen dynamics reflect organic inputs via the extended composite phenotype. *Nature Food*, *4*(1), 51–60. https://doi.org/10.1038/s43016-022-00671-z

Oksanen, J., Simpson, G., Blanchet, F., Kindt, R., Legendre, P., Minchin, P., et al. (2024). Vegan: Community ecology package. *R package version 2.6-6.1*. https://CRAN.R-project.org/package=vegan

Philippot, L., Chenu, C., Kappler, A., Rillig, M. C., & Fierer, N. (2024). The interplay between microbial communities and soil properties. *Nature Reviews Microbiology*, *22*(4), 226–239. https://doi.org/10.1038/s41579-023-00980-5

Põlme, S., Abarenkov, K., Henrik Nilsson, R., Lindahl, B. D., Clemmensen, K. E., Kauserud, H., et al. (2021). Correction to: Fungaltraits: A user friendly traits database of fungi and fungus-like stramenopiles. *Fungal Diversity*, *107*(1), 129–132. https://doi.org/10.1007/s13225-021-00470-0

Rahmati, M., Or, D., Amelung, W., Bauke, S. L., Bol, R., Hendricks Franssen, H. J., et al. (2023). Soil is a living archive of the Earth system. *Nature Reviews Earth & Environment*, *4*(7), 421–423. https://doi.org/10.1038/s43017-023-00454-5

Rousk, J., Bååth, E., Brookes, P. C., Lauber, C. L., Lozupone, C., Caporaso, J. G., et al. (2010). Soil bacterial and fungal communities across a ph gradient in an arable soil. *The ISME Journal*, *4*(10), 1340–1351. https://doi.org/10.1038/ismej.2010.58

Sebilo, M., Mayer, B., Nicolardot, B., Pinay, G., & Mariotti, A. (2013). Long-term fate of nitrate fertilizer in agricultural soils. *Proceedings of the National Academy of Sciences*, *110*(45), 18185–18189. https://doi.org/10.1073/pnas.1305372110

Smerald, A., Fuchs, K., Kraus, D., Butterbach-Bahl, K., & Scheer, C. (2022). Significant global yield-gap closing is possible without increasing the intensity of environmentally harmful nitrogen losses. *Frontiers in Sustainable Food Systems*, *6*, 736394. https://doi.org/10.3389/fsufs.2022.736394

Smerald, A., Kraus, D., Rahimi, J., Fuchs, K., Kiese, R., Butterbach-Bahl, K., & Scheer, C. (2023). A redistribution of nitrogen fertiliser across global croplands can help achieve food security within environmental boundaries. *Communications Earth & Environment*, *4*(1), 315. https://doi.org/10.1038/s43247-023-00970-8

Stefanowicz, A. M., Niklińska, M., & Laskowski, R. (2008). Metals affect soil bacterial and fungal functional diversity differently. *Environmental Toxicology and Chemistry*, *27*(3), 591–598. https://doi.org/10.1897/07-288.1

Steffen, W., Richardson, K., Rockström, J., Cornell, S. E., Fetzer, I., Bennett, E. M., et al. (2015). Planetary boundaries: Guiding human development on a changing planet. *Science*, *347*(6223), 1259855. https://doi.org/10.1126/science.1259855

Stevens, C. J. (2019). Nitrogen in the environment. *Science*, *363*(6427), 578–580. https://doi.org/10.1126/science.aav8215

Tian, H., Pan, N., Thompson, R. L., Canadell, J. G., Suntharalingam, P., Regnier, P., et al. (2024). Global nitrous oxide budget (1980–2020). *Earth System Science Data*, *16*(6), 2543–2604. https://doi.org/10.5194/essd-16-2543-2024

Tian, X. (2025). Resistance and recovery of crop productivity from contrasted soil fertility [Dataset]. *Zenodo*. https://doi.org/10.5281/zenodo.17299196

Tian, X., Zhang, C., & Ju, X. (2023). Crop responses to application of optimum nitrogen fertilizers on soils of various fertilities formed from long-term fertilization regimes. *European Journal of Agronomy*, *148*, 126857. https://doi.org/10.1016/j.eja.2023.126857 van der Velde, M., Folberth, C., Balkovič, J., Ciais, P., Fritz, S., Janssens, I. A., et al. (2014). African crop yield reductions due to increasingly unbalanced nitrogen and phosphorus consumption. *Global Change Biology*, *20*(4), 1278–1288. https://doi.org/10.1111/gcb.12481

van Dijk, M., Morley, T., Rau, M. L., & Saghai, Y. (2021). A meta-analysis of projected global food demand and population at risk of hunger for the period 2010–2050. *Nature Food*, *2*(7), 494–501. https://doi.org/10.1038/s43016-021-00322-9

Wang, C., Shen, Y., Fang, X., Xiao, S., Liu, G., Wang, L., et al. (2024). Reducing soil nitrogen losses from fertilizer use in global maize and wheat production. *Nature Geoscience*, *17*(10), 1008–1015. https://doi.org/10.1038/s41561-024-01542-x

Wang, X., Feng, J., Ao, G., Qin, W., Han, M., Shen, Y., et al. (2023). Globally nitrogen addition alters soil microbial community structure, but has minor effects on soil microbial diversity and richness. *Soil Biol. Biochem.*, *179*, 108982. https://doi.org/10.1016/j.soilbio.2023.108982

Wang, Z., Yin, Y., Wang, Y., Tian, X., Ying, H., Zhang, Q., et al. (2022). Integrating crop redistribution and improved management towards meeting china's food demand with lower environmental costs. *Nature Food*, *3*(12), 1031–1039. https://doi.org/10.1038/s43016-022-00646-0

Wen, Z., Xu, W., Li, Q., Han, M., Tang, A., Zhang, Y., et al. (2020). Changes of nitrogen deposition in China from 1980 to 2018. *Environment International*, *144*, 106022. https://doi.org/10.1016/j.envint.2020.106022

Wickham, H., Averick, M., Bryan, J., Chang, W., McGowan, L., François, R., et al. (2019). Welcome to the tidyverse. *Journal of Open Source Software*, *4*(43), 1686. https://doi.org/10.21105/joss.01686

Xiao, L., Wang, G., Wang, E., Liu, S., Chang, J., Zhang, P., et al. (2024). Spatiotemporal co-optimization of agricultural management practices towards climate-smart crop production. *Nature Food*, *5*(1), 59–71. https://doi.org/10.1038/s43016-023-00891-x

Xu, P., Li, G., Zheng, Y., Fung, J. C. H., Chen, A., Zeng, Z., et al. (2024). Fertilizer management for global ammonia emission reduction. *Nature*, *626*(8000), 792–798. https://doi.org/10.1038/s41586-024-07020-z

Xu, Q., Li, L., Guo, J., Guo, H., Liu, M., Guo, S., et al. (2024). Active microbial population dynamics and life strategies drive the enhanced carbon use efficiency in high-organic matter soils. *mBio*, *15*(3), e00177-24. https://doi.org/10.1128/mbio.00177-24

Yan, M., Pan, G., Lavallee, J. M., & Conant, R. T. (2020). Rethinking sources of nitrogen to cereal crops. *Global Change Biology*, *26*(1), 191–199. https://doi.org/10.1111/gcb.14908

Yan, Y., Zhou, X., Liu, L., Cai, Z., Penuelas, J., & Huang, X. (2025). Soil nutrient enrichment induces trade-offs in bacterial life-history strategies promoting plant productivity. *Advanced Science*, *12*(45), e10066. https://doi.org/10.1002/advs.202510066

Yang, Y., Chen, X., Li, T., Liu, L., Dou, Y., Qiao, J., et al. (2022). Nitrogen fertilization weakens the linkage between soil carbon and microbial diversity: A global meta-analysis. *Global Change Biology*, *28*(21), 6446–6461. https://doi.org/10.1111/gcb.16361

Yin, Y., Zhao, R., Yang, Y., Meng, Q., Ying, H., Cassman, K. G., et al. (2021). A steady-state n balance approach for sustainable smallholder farming. *Proceedings of the National Academy of Sciences of the United States of America*, *118*(39), e2106576118. https://doi.org/10.1073/pnas.2106576118

Zhan, X., Adalibieke, W., Cui, X., Winiwarter, W., Reis, S., Zhang, L., et al. (2020). Improved estimates of ammonia emissions from global croplands. *Environmental Science and Technology*, *55*(2), 1329–1338. https://doi.org/10.1021/acs.est.0c05149

Zhang, C., Ju, X. T., Powlson, D., Oenema, O., & Smith, P. (2019). Nitrogen surplus benchmarks for controlling n pollution in the main cropping systems of China. *Environmental Science and Technology*, *53*(12), 6678–6687. https://doi.org/10.1021/acs.est.8b06383

Zhang, C., Rees, R. M., & Ju, X. T. (2021). Fate of n-15-labelled urea when applied to long-term fertilized soils of varying fertility. *Nutrient Cycling in Agroecosystems*, *121*(2–3), 151–165. https://doi.org/10.1007/s10705-021-10166-1

Zhang, X., Davidson, E., Mauzerall, D., Searchinger, T. D., Dumas, P., & Shen, Y. (2015). Managing nitrogen for sustainable development. *Nature*, *528*(7580), 51–59. https://doi.org/10.1038/nature15743

Zhao, X., Wang, Y., Cai, S., Ladha, J. K., Castellano, M. J., Xia, L., et al. (2024). Legacy nitrogen fertilizer in a rice-wheat cropping system flows to crops more than the environment. *Scientific Bulletin*, *69*(9), 1212–1216. https://doi.org/10.1016/j.scib.2024.02.027

References From the Supporting Information

INFS (Institute of Nutrition and Food Safety). (2005). *China CDC 2005, China Food Composition 2004*. Peking University Medical Press. (in Chinese).

Liang, B., Zhao, W., Yang, X., & Zhou, J. (2013). Fate of nitrogen-15 as influenced by soil and nutrient management history in a 19-year wheat-maize experiment. *Field Crops Research*, *144*, 126–134. https://doi.org/10.1016/j.fcr.2012.12.007

NBSC (National Bureau of Statistics of China). (2024). National data. Retrieved from https://data.stats.gov.cn/

Swarbreck, S. M., Wang, M., Wang, Y., Kindred, D., Sylvester-Bradley, R., Shi, W., et al. (2019). A roadmap for lowering crop nitrogen requirement. *Trends in Plant Science*, *24*(10), 892–904. https://doi.org/10.1016/j.tplants.2019.06.006

UN (United Nations). (2024). World Population Prospects 2024: Data sources. (UN DESA/POP/2024) Retrieved from https://population.un.org/wpp/

USDA (United States Department of Agriculture). (2024). *Foreign Agricultural Service*. Retrieved from https://apps.fas.usda.gov/psdonline/app/index.html#/app/advQuery

Zörb, C., Ludewig, U., & Hawkesford, M. J. (2018). Perspective on wheat yield and quality with reduced nitrogen supply. *Trends in Plant Science*, *23*(11), 1029–1037. https://doi.org/10.1016/j.tplants.2018.08.012